

Fig. 4.15 – Fault crossing the Dalton Pass road at km 199+300 (top), at km 201+300 (center) and at km 201+400 (bottom). Courtesy of DPWH and Katahira.

4.6. The analysis of the earthquake

4.6.1 Data recording and processing

Seismographs in Luzon went off-scale about 45 seconds after the July 16, 1990 ground shaking began, thus earthquake analysis was based on data from outside the Philippines. In particular, seismic signals recorded at three stations in Italy, and made available by the Istituto Nazionale di Geofisica (ING), were used. These Broad Band Stations, under the ING, are part of the Mediterranean Network (MedNet) recently established for monitoring the seismicity in the area (MedNet Workshop, 1990). The system has the advantage of providing an undistorted signal, linear over a very large frequency range. The broad-band signal is digitally sampled from the seismometer and recorded on magnetic tape. The technique was developed in the USA in 1962 (Wielandt, 1991) and the first European seismological station came into operation in 1976 in Germany. The signal of the earthquake can be used for advanced data-processing based on mathematical modelling and the spatial and temporal distribution of the seismic source can be derived along with seismic parameters.

Ground displacement was retrieved first by integrating the broad-band signal (Fig. 4.17) recorded at the Italian stations; then, the characteristics of the ground rupture were determined (Morelli, 1991; Giardini, 1991) through a mathematical procedure based on ray-theory. The earthquake signal was thus decoded and the source-time function and the focal mechanism derived.

A broad comparison was attempted of the initial 230 seconds of ground shaking (time intervals A + B in the lower seismogram of Fig. 4.17) and eyewitness information (Para. 4.5). The first shock that people felt appears to lie within the initial 120 sec shock in the record (time interval A, in Fig. 4.17, bottom). The following pause which reportedly lasted 174 seconds can be partly identified in the seismogram as a clear drop in ground shaking for about 110 seconds (time interval B). The arrival of PP waves at 230 seconds prevents any further attempts at comparison; thus, the second shock with probable epicenter in Kayapa (Fig. 4.1), cannot be identified, due to overlapping of signal and PP waves.

4.6.2 Seismic source analysis

Seismic records from distant stations can thus be used to search for the focal mechanism and source-time function by appropriate mathematical processing. The trace in Figure 4.17 (upper seismogram) shows the Luzon earthquake signal (vertical ground-shaking P wave component) as recorded at L'Aquila Station in Italy. An enlarged detail of the initial 1440 seconds is shown in the lower sketch, with indications of first arrivals of P, PP, S and PKIKP waves. In Figure 4.18 a cross-section of the globe illustrates different travel paths including those related to the four mentioned wave types, while arrival times are shown in the sketch on the right for different angles between the focus, the center of the earth and the receiving station.

In the case of the July 1990 earthquake, a 92 degree angle between the source (Luzon epicenter) and the receiving station (L'Aquila) was used. The cross-section in Figure 4.18 (left) shows the variety of waves (conventionally indicated by capital letters and combinations depending on trajectories) which can arrive at a recording station located at progressively greater distances from the source. The inner core, outer core and mantle play major roles in this respect by reflecting, refracting and diffracting P waves, while the molten outer core entirely blocks S waves. The duration of the seismogram (Fig. 4.17, top) depends on the location of the epicenter with respect to the receiving station and on the type of recording instrumentation: it does not provide any information regarding the shaking time in the epicentral area.

To return to the determination of source parameters, Figure 4.19 illustrates the focal mechanism and source-time function retrieved through the analysis based on ray theory. In detail, the full lines in graphs on the left represent data derived by integrating recorded seismic signals at the three Italian MedNet stations of Villasalto (VSL), Bardonecchia (BNI) and L'Aquila (AQU). Dotted lines show traces derived through the simulation procedure for generating synthetic seismograms. The simulation process is based on four time-domain functions representative of phenomena accompanying seismic wave propagation and on the model assumption of horizontally layered media (Beranzoli et al., 1993).

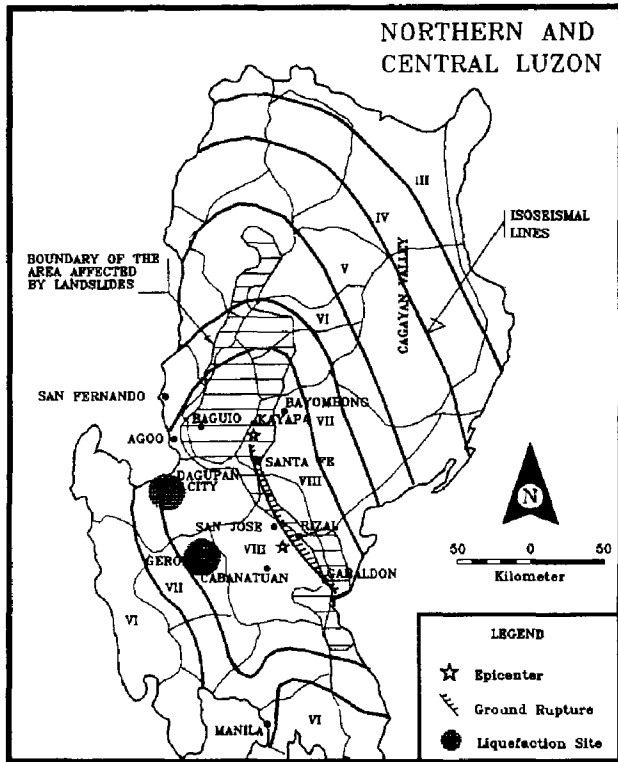


Fig. 4.16 - Earthquake Intensity Map based on the Rossi-Forel Scale (Appendix C). Adapted from Punnongbayan and Torres (1990).

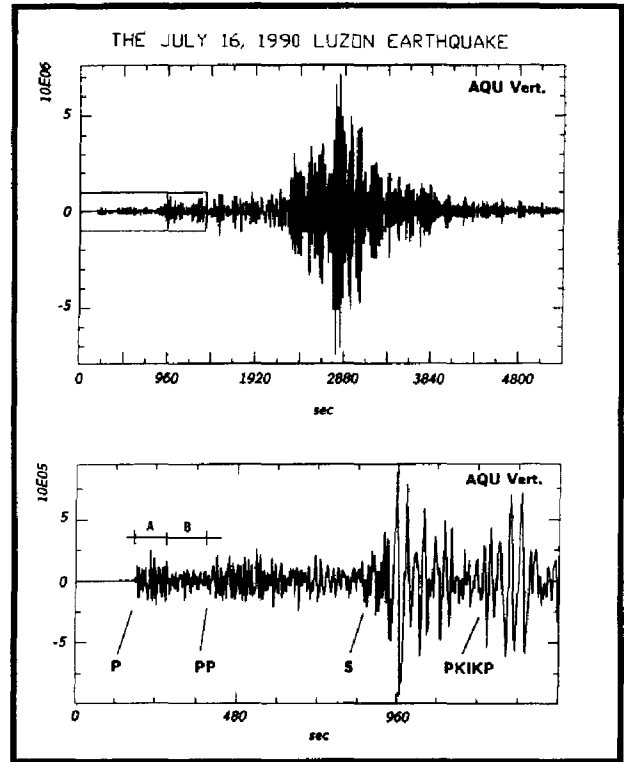


Fig. 4.17 - Seismogram of the July 16, 1990 Luzon earthquake (top), recorded at the station of L'Aquila (Central Italy). The lower sketch represents the enlarged portion of the above seismogram for the initial 1440 seconds (Istituto Nazionale di Geofisica, Rome, Italy).

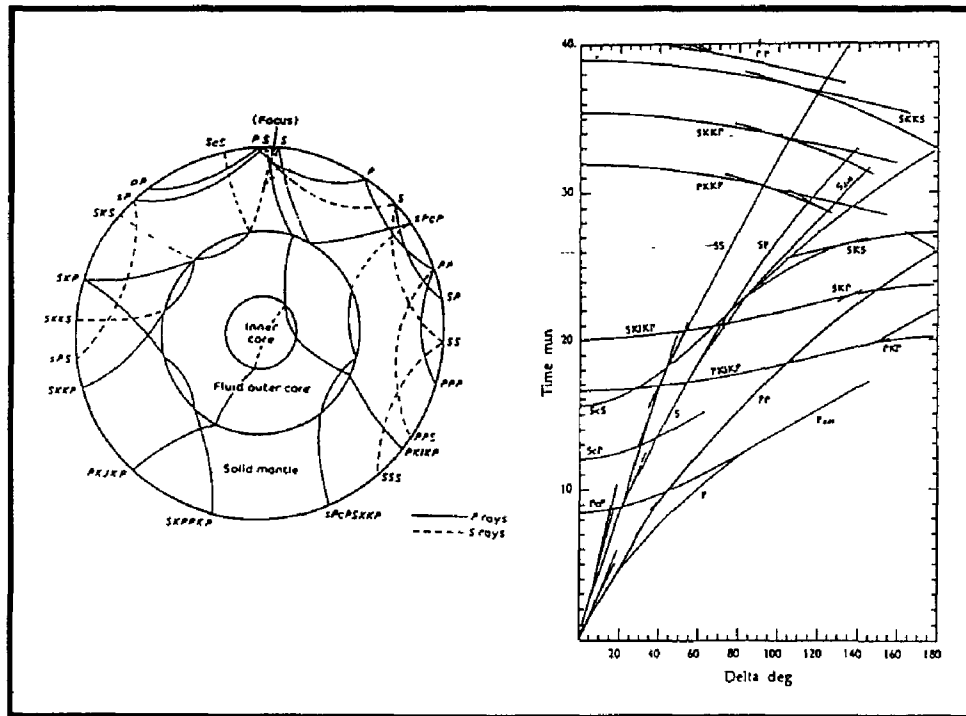


Fig. 4.18 - The cross-section of the earth illustrates travel paths of different waves originating from the quake focus. Waves are conventionally indicated by capital letters depending on trajectories. The sketch on the right shows the arrival time of these waves as a function of the angle between the focus, the center of the earth and the receiving station.

In the three 150-second sketches of Figure 4.19, synthetic seismograms (dotted lines) are in good agreement with the traces derived from recorded data. This is interpreted as a successful simulation and, therefore, correct identification of the focal mechanism and source-time function. The upper right-hand sketch in the same Figure shows the focal mechanisms, which is illustrated by the equal area projection of the lower hemisphere of the focal sphere. The plane with N147E strike (and SW dip at an angle of 62 degrees) coincides with the direction of the major ground rupture trace along the Philippine Fault near Rizal City (Fig. 4.1), where the first epicenter was located.

The lower-right sketch in Fig. 4.19, which shows the source-time function, indicates that the first major shock was composed of three sub-events for an overall duration of 120 seconds.

Combining recorded data and eyewitness information, the Luzon earthquake was most probably generated by two major shocks, separated by a lower seismicity level which lasted over 120 seconds. The first event (composed of three sub-events) occurred at a depth of 24.8 km; the second epicenter, based on eyewitness reports and damage assessment, can be located near Kayapa, some 30 km E of Baguio.

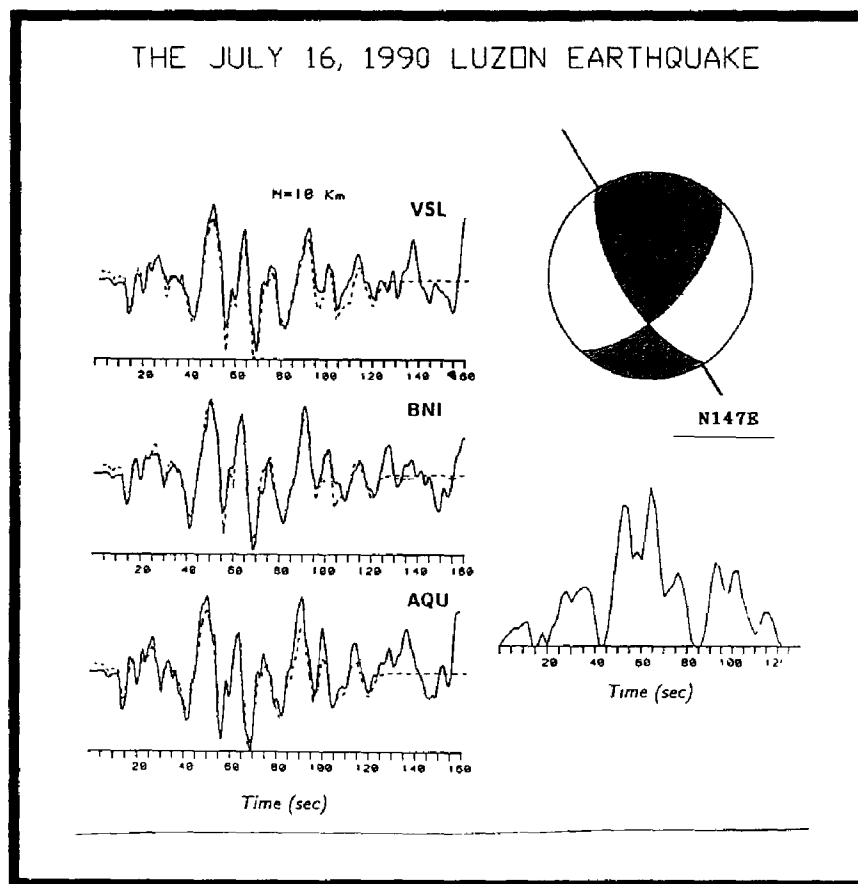


Fig. 4.19 – Data processing and interpretation, Focal Mechanism Solution and Source Time Function. The sketches on the left show full lines derived from data recorded at the Italian stations of Villasalto, Bardonecchia and L'Aquila, and dotted lines from synthetic seismograms. The agreement between the two is an indication of successful simulation. The equal area projection at top right shows that the identified focal mechanism is of the strike-slip type, and that the predominant direction of motion is lateral. Since the plane with strike N147E (and dip SW 62°) coincides fairly well the direction of the major ground rupture near Rizal (Fig. 4.1) where the epicenter was located, it is interpreted as the fault plane. Dashed and blank zones (bounded by the fault plane and the auxiliary plane) represent compressional and dilatational first motions, respectively, and their position indicates that the motion was mainly left lateral. The lower sketch, the source-time function, shows that the first major shock was composed of three subevents for an overall duration of 120 seconds (Istituto Nazionale di Geofisica, Italy).

4.7 Damage distribution and subsurface rearrangement

The earthquake caused limited damage in the epicentral area in comparison to Baguio City and the towns along Lingayen Gulf where damage was severe. The destructive effect of the earthquake on the zone west of the ground rupture was exacerbated by the countless landslides which affected the Caraballo Mountains and the Central Cordillera.

In general the damage extended along the ground rupture zone and west of it through the Cordillera. By contrast, the Cagayan River Valley and Sierra Madre Range were marginally involved. According to Sharp (USGS-PHIVOLCS Report, 1990) «the jerky propagation of the rupture and its northwestward trend might have resulted at some degree in an attenuation of the seismic waves in the eastern block and amplification in the western region». The seismic swarm which followed the quake (Chapter 7) is thought to be related to the compression induced in western Luzon by the 1990 slip. Through a sizable subsurface block readjustment and numerous aftershocks the accumulated stress was released mainly during the period July-October 1990.

One reason for the underground rearrangement was probably that it was difficult for the Cordillera to absorb the compression, due to the presence of deep rooted, massive batholiths with limited and complex displacement potential along the various intersecting lineaments. The block's reassemblage (after the July 1990 quake) was most probably coupled with some uplift of the Cordillera.

4.8 Recurrence period

Based on an average displacement of 2 cm/year along the Philippine Fault, the July 1990 horizontal slip of 6.2 m probably compensated about 310 years of stress accumulation. The last strong earthquake in the same area occurred in 1645, 345 years before the 1990 event. According to Newhall (USGS-PHIVOLCS Report, 1990), however, historical records of the 1645 earthquake mainly deal with Manila, thus the location of this event along the Gabaldon-Rizal segment of the Philippine Fault is uncertain.

The Philippine Fault in Central Luzon splits into a number of splays which can accommodate the crustal shortening along different segments moving at different times. The presence in Central Luzon of other earthquake generators makes the problem even more complex. Some progress in forecasting the probable location of the next strong earthquake in the Central-Northern Luzon region could probably be achieved through further analysis of data and locations of past earthquakes and the movements along active faults.

4.9 Casualties, damage and environmental impact

4.9.1 General

The earthquake intensity map shown in Fig 4.16 gives a general indication of damage distribution in Luzon. Consequences of the 1990 earthquake can be considered under four headings: human losses and injuries; damage to property, infrastructure and services; environmental impact; and the economic damage to the Philippines (described in Chapter 9).

4.9.2 Human losses

There were 1,666 deaths, about 1,000 persons were reported missing and over 3,000 were injured. Most casualties occurred in Baguio City and surroundings. The maximum intensity, VIII, regarded the area between Kayapa, Gabaldon, Tarlac, Dagupan, Agoo and Baguio (Fig. 4.16). A sizable part of the mountainous zone affected by intensities VI and VII is sparsely inhabited so casualties were relatively few. In Metro Manila, where the intensity was VI to VII, people in Makati were terrified by skyscraper oscillations, but no casualties were reported, although numerous old buildings were damaged. Due to the disruption of the road network it took days for the rescue teams to reach some remote areas.

The rainy season, which began soon after the tremor, produced new casualties, some as the result of reactivation of earthquake-induced slides and some because of new slope movements generated by the rains.

4.9.3 *Damage to property and infrastructure*

Nearly 100,000 houses suffered damage and 40% of them were virtually destroyed. Figure 4.11 is a location map of the area most severely affected by the quake and Figure 4.20 illustrates some striking examples of structural damage in Baguio where a number of hotels and buildings collapsed. Towns in the coastal area south of San Fernando in La Union, along the Lingayen Gulf and in the area between Dagupan and Tarlac (Chapter 5), were damaged by extensive liquefaction. A six storey school collapsed in Cabanatuan, near the epicenter

Damage to agriculture was mainly limited to the irrigation and drainage system in the area along the ground rupture zone. Due to the vertical displacement along the Fault, the gradients of channels were upset, thus disrupting regular operation of the irrigation network. The supply of crops from the Cagayan River Valley to Manila was subject to delays because of damage to Dalton Pass Road. Additional problems occurred later because of the heavy rains which resulted in the road being threatened by slides for months.

Seven bridges collapsed, eight were seriously damaged and about 20 were affected by various types of lesser damage. Major bridges that were destroyed included the 600-m long truss bridge over the Agno River in Plaridel (Fig. 4.21, bottom) and the five-span Magsaysay concrete bridge in Dagupan City (Figs. 5.2 and 5.10), both of which collapsed due to liquefaction. Many bridge abutments were damaged, approaches suffered marked settlement and piers suffered tilting or settlement.

The road network of Central Luzon (Fig. 4.11) and the Baguio region (JICA Report, 1990) was significantly damaged by the quake. Roads in mountainous areas (Figs. 4.21 top and 6.5) suffered damage due to cut-slope and embankment failures, longitudinal cracks, pavement deformation, differential settlement of fills. Marcos Highway in particular and Kennon Road (along the Agno River), both leading to Baguio City (Fig. 4.11) were largely destroyed by landslides. A segment of Marcos Highway near Baguio, along a very steep hillside, slid down the slope. The situation was made even worse by the onset of the rainy season (Chapter 6). Naguillian and Halsema Roads near Baguio were seriously affected by huge joint-controlled rock slides, mainly through plane failures of sandstone formations. A section of the Maharlika Highway through the Caraballo Mountains (Figs. 4.13 - 4.15) suffered enormous damage.

Roads in the Central Plain, between Dagupan and Tarlac and near Lingayen Gulf, were badly affected by liquefaction-induced effects. The most common features were long longitudinal cracks, waviness of the road bed, separation of shoulders, disruption of the concrete pavement and generalized disintegration of embankments due to the dissipation of the excess pore-water pressure during liquefaction (Chapter 5).

About 60 km north of Manila along the North Super Highway cement concrete girders of a viaduct were displaced about 80 cm with respect to the bridge centerline.

Dams were also damaged in various ways (JICA Report, 1990). Crest settlement occurred at Ambuklao, Binga, Mastway and Pantabangan Dams, the first two about 15 km east of Baguio City, and the second two 10 km east of San Jose' and about the same distance from the first epicenter, near Rizal City (Fig. 4.11). Cracks and landslides were observed in various parts of the basins and along crests.

Ambuklao Dam was silted up to a few meters below water level with an estimated 60 million cubic meters of sediments, a considerable part of which were transported during the two months after the quake. According to the design the dam should have had a useful life of 50 years before complete siltation, but the effects of the quake contributed to shorten this period to a mere 28 years.

River facilities, parapets, and protective structures in general suffered widespread damage due to ground shaking or to lateral spreading induced by liquefaction. Of the public utilities the electricity network was the most badly hit. Numerous poles were tilted and the electricity supply was interrupted for days, and even weeks in some of the remotest areas. Sewerage networks in cities affected by liquefaction were almost entirely disrupted.



Fig. 4.20 – Badly damaged buildings in Baguio City (top, FRB Hotel and Royal Inn, bottom, Hilltop and Nevada Hotels).

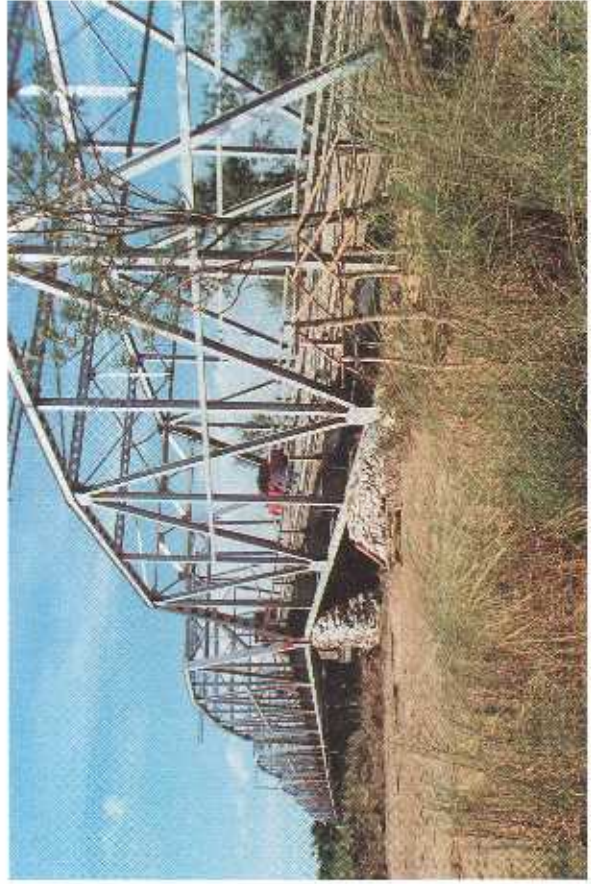


Fig. 4.21 – Damaged sections of the Dalton Pass Road at km 203 + 250 (top left) and at km 200 + 750 (top right), Courtesy of DPWH and Katahira. The collapsed Platidel Truss Bridge, over the Agno River, in Carmen (Rosales), about 60 km North of Tarlac (bottom).



Fig. 4.22 – The overtopped Puncan Bridge along the Dalton Pass Road at km 177.

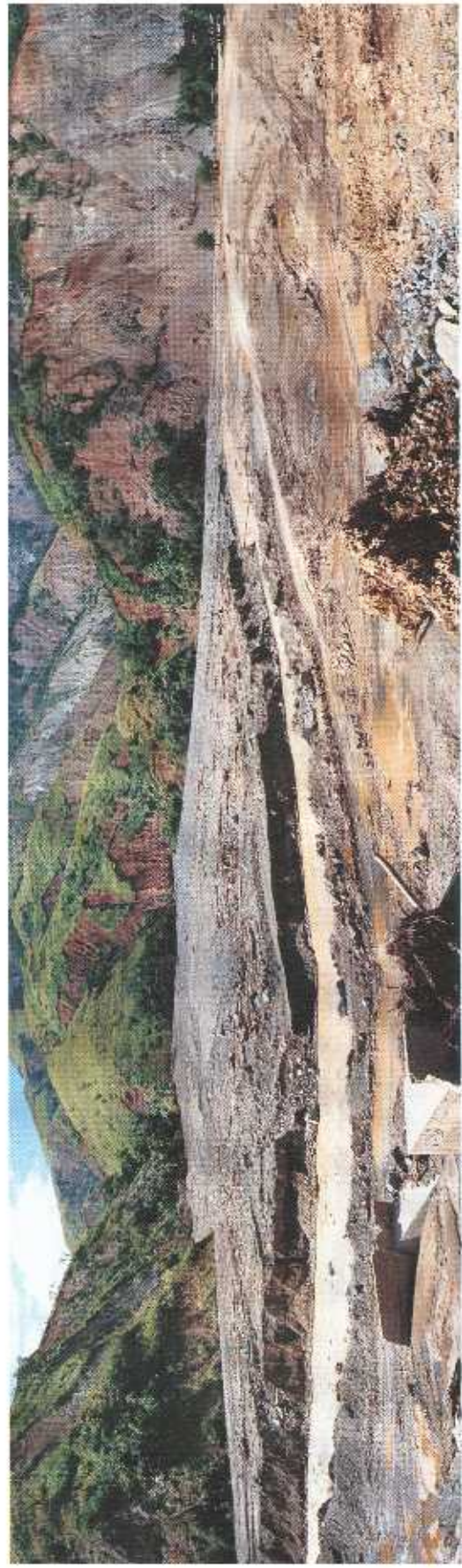


Fig. 4.23 – Fan of newly deposited sediments and debris along the Dalton Pass Road.

4.9.4 *Environmental impact*

The damage by the quake to the environment consisted mainly of innumerable slides and the destruction of the vegetation cover in the slide areas. Within a narrow strip along the rupture lines the ground surface was visibly broken for over 175 km. Associated effects included landslides, liquefaction, accelerated erosion and further downslope movements of materials loosened by the quake and mobilized again by the rains.

Landslide areas included the mountainous regions of Western and Central Luzon, namely the middle and southern parts of the Central Cordillera and the whole of the Caraballo Mountains. The slides destroyed numerous trees, both where the surface material was mobilized and downslope, where they were covered by debris.

Figure 4.22 illustrates the extent of the damage through the huge quantity of trees which accumulated by August 1990 at Puncan Bridge along the Dalton Pass Road. The numerous slides in mountainous provinces contributed to the uprooting of vegetation on steep slopes where human-induced deforestation had proved impractical. Extensive alluvial fans (Fig. 4.23), produced by accelerated erosion, formed along major rivers and near the periphery of mountains.